

Cosmology in the Next Millennium: Combining MAP and SDSS Data to Constrain Inflationary Models

Yun Wang, David N. Spergel, & Michael A. Strauss^{1,2}

Princeton University Observatory

Peyton Hall, Princeton, NJ 08544

email: ywang,dns,strauss@astro.princeton.edu

Abstract

The existence of primordial adiabatic Gaussian random-phase density fluctuations is a generic prediction of inflation. The properties of these fluctuations are completely specified by their power spectrum $A_S^2(k)$. The basic cosmological parameters and the primordial power spectrum together completely specify predictions for the cosmic microwave background radiation anisotropy and large scale structure. Here we show how we can strongly constrain both $A_S^2(k)$ and the cosmological parameters by combining the data from the Microwave Anisotropy Probe (MAP) and the galaxy redshift survey from the Sloan Digital Sky Survey (SDSS). We allow $A_S^2(k)$ to be a free function, and thus probe features in the primordial power spectrum on all scales. If we assume that the cosmological parameters are known *a priori* and that galaxy bias is linear and scale-independent, and neglect non-linear redshift distortions, the primordial power spectrum in 20 steps in $\log k$ to $k \leq 0.5h\text{Mpc}^{-1}$ can be determined to $\sim 16\%$ accuracy for $k \sim 0.01h\text{Mpc}^{-1}$, and to $\sim 1\%$ accuracy for $k \sim 0.1h\text{Mpc}^{-1}$. The uncertainty in the primordial power spectrum increases by a factor up to 3 on small scales if we solve simultaneously for the dimensionless Hubble constant h , the cosmological constant Λ , the baryon fraction Ω_b , the reionization optical depth τ_{ri} , and the effective bias between the matter density field and the redshift space galaxy density field b_{eff} . Alternately, if we restrict $A_S^2(k)$ to be a power law, we find that inclusion of the SDSS data breaks the degeneracy between the amplitude of the power spectrum and the optical depth inherent in the MAP data, significantly reduces the uncertainties in the determination of the matter density and the cosmological constant, and allows a determination of the galaxy bias parameter. Thus, combining the MAP and

¹Alfred P. Sloan Foundation Fellow

²Cottrell Scholar of Research Corporation

SDSS data allows the independent measurement of important cosmological parameters, and a measurement of the primordial power spectrum independent of inflationary models, giving us valuable information on physics in the early Universe, and providing clues to the correct inflationary model.

1. Introduction

Standard cosmology poses three basic conundrums: why the universe is homogeneous on large scales, why the cosmological density parameter Ω_m is close to unity, and what seeds the large-scale structure in the universe. Inflation provides compelling solutions to all these problems (Kolb & Turner 1990).

The cosmic microwave background radiation (CMB) is observed to be isotropic to an accuracy of better than 10^{-4} . This implies that the Universe was homogeneous to this accuracy over many horizon scales at last scattering. Within the standard cosmology there is no causal process which could have created the observed homogeneity. The basic idea of inflation is that the observable Universe grew from an initial patch small enough to fit inside the horizon. It is hypothesized that there were particle physics mechanisms which led to the rapid expansion of the early Universe required to produce the huge growth factor necessary to solve the cosmological problems above. In this paper, we assume that inflation produces primordial adiabatic Gaussian random-phase density fluctuations due to quantum fluctuations in the inflaton field. The properties of these fluctuations are completely specified by their power spectrum $A_S^2(k)^3$. This paper will emphasize how well the shape of the primordial power spectrum can be measured from CMB anisotropy and redshift survey data.

There currently exists a broad range of inflationary models (Kolb 1997, Turner 1997). Some of these models predict power spectra that are almost exactly scale-invariant (Linde 1983), or are described by a power law with spectral index less than one (Freese, Frieman, & Olinto 1990, La & Steinhardt 1991), while others predict power spectra with slowly varying spectral indices (Wang 1994), or with broken scale invariance (Holman et al. 1991ab, Adams, Ross, & Sarkar 1997, Lesgourgues, Polarski, & Starobinsky 1997).

Indeed, there are physical reasons to believe that the primordial power spectrum has breaks in its power-law form. In effective (i.e., not complete) theories with two scalar fields, inflation may occur in two stages. The two stages of inflation can generate density perturbations with different power-law indices, with a step in amplitude of the primordial power spectrum on the scale of the transition between the two phases (Holman et al. 1991ab). Fry & Wang (1992) found that such models can have a significant signature on small-scale CMB anisotropies.

Recently, Adams, Ross, & Sarkar (1997) proposed a new multiple inflation model. Since

³Certain two-field inflationary models predict isocurvature as well as adiabatic fluctuations (Kofman & Linde 1987). Since the CMB and LSS predictions of isocurvature models differ significantly from adiabatic models and since these differences are not degenerate with parameter variation, we could, in principle, also fit for an isocurvature power spectrum. However, in this paper, we limit ourselves to considering adiabatic fluctuations.

attempts at an unified description of the strong, weak and electromagnetic interactions usually involve several stages of spontaneous symmetry breaking, they considered the effects of such symmetry breaking during an era of inflation in supergravity models. They found that there can be a succession of short bursts of inflation; the density perturbations produced during each burst is nearly scale-invariant but with differing amplitudes, and between each burst there is a brief period during which scale-invariance is badly broken.

Given the range of possibilities for the primordial power spectrum, we would like to quantify how well it can be measured generically. Thus, we take the primordial power spectrum to be a free function in this paper.

The upcoming data from the Microwave Anisotropy Probe (MAP; cf., Bennett et al. 1997; <http://map.gsfc.nasa.gov>) and the Sloan Digital Sky Survey (SDSS; cf., Gunn & Weinberg 1996) provide a unique opportunity for constraining inflationary models. It is useful to expand the temperature fluctuations in the CMB into spherical harmonics: $\delta T/T(\hat{\mathbf{r}}) = \sum_{l,m} a_{T,lm} Y_{lm}(\hat{\mathbf{r}})$, where $\hat{\mathbf{r}}$ is the unit direction vector in the sky. MAP measures the angular power spectrum (Seljak & Zaldarriaga 1996)

$$C_{Tl} \equiv \langle |a_{T,lm}|^2 \rangle = (4\pi)^2 \int \frac{dk}{k} A_S^2(k) |\Delta_{Tl}(k, \tau = \tau_0)|^2, \quad (1)$$

where $A_S^2(k)$ is the power spectrum of the primordial density fluctuations (defined such that $A_S^2(k) = 1$ for the scale-invariant Harrison-Zel'dovich spectrum), $\Delta_{Tl}(k, \tau = \tau_0)$ is an integral over conformal time τ of the sources which generate the CMB fluctuations, and τ_0 is the conformal time today.

The power spectrum of mass fluctuations in the linear regime today is

$$P(k) = P_0 k A_S^2(k) T^2(k), \quad (2)$$

where P_0 is a normalization constant, and $T(k)$ is the transfer function, which depends on physics at matter-radiation equality and decoupling. Note that P_0 has been absorbed into the definition of $\Delta_{Tl}(k, \tau = \tau_0)$ in Eq. (1).

The galaxy redshift survey from the SDSS (cf., Strauss 1997 for a description) will allow a determination of $P_G(k)$, the galaxy power spectrum in redshift space. The quantity $P_G(k)$ differs from the mass power spectrum $P(k)$ due to two effects. First, the galaxy distribution may be biased with respect to the mass distribution. On large scales, models (Weinberg 1995; Kauffmann, Nusser, & Steinmetz 1997; Scherrer & Weinberg 1997) indicate that the mass and galaxy density fields are directly proportional to one another. The proportionality constant is referred to as the galaxy bias parameter, b . Second, peculiar velocities cause the density contrast of galaxies in redshift space to appear appreciably stronger than in real space. In linear theory, the power spectrum is boosted by a factor $1 + \frac{2}{3}\beta + \frac{1}{5}\beta^2$, where $\beta \equiv \Omega_m^{0.6}/b$ (Ω_m is the matter density in units of the critical density of the Universe $\rho_c \equiv 3H_0^2/(8\pi G)$, with H_0 denoting the Hubble constant). The net result (Kaiser 1987; cf.,

(Hamilton 1998 for a review) is that on linear scales, the galaxy power spectrum is given by:

$$P_G(k) = b^2 \left(1 + \frac{2}{3}\beta + \frac{1}{5}\beta^2 \right) P(k) \equiv b_{\text{eff}}^2 P(k). \quad (3)$$

The observables C_{Tl} and $P_G(k)$ depend on the cosmological parameters H_0 , Ω_b (baryon density in units of ρ_c), Ω_m , Ω_Λ (density contribution from the Cosmological Constant in units of ρ_c), and τ_{ri} (reionization optical depth) only through $\Delta_{Tl}(k, \tau = \tau_0)$, b_{eff} , and $T(k)$. The MAP data alone will allow rather tight constraints on the baryon/photon ratio (which determines $\Omega_b h^2$), the matter/photon ratio (which determines $\Omega_m h^2$), and the geometry of the universe, and test the basic inflationary scenario (Spergel 1994; Knox 1995; Jungman et al. 1996; Bond, Efstathiou & Tegmark 1997; Zaldarriaga, Spergel & Seljak 1997; Dodelson, Kinney & Kolb 1997; Lidsey et al. 1997; Copeland, Grivell & Liddle 1997; Efstathiou & Bond 1998; Eisenstein, Hu & Tegmark 1998). However, there is a near-degeneracy in several sets of parameters (Bond et al. 1994; Bond, Efstathiou & Tegmark 1997; Zaldarriaga, Spergel & Seljak 1997; Huey & Dave 1997) including the overall amplitude of the power spectrum at $k \sim 0.1 h\text{Mpc}^{-1}$ and the optical depth. Since $\Delta_{Tl}(k, \tau = \tau_0)$ and $T(k)$ depend on the cosmological parameters differently, by combining the MAP and SDSS data, we can break these degeneracies and determine cosmological parameters to impressive accuracies. Several other recent papers have also considered how well cosmological parameters can be constrained with the combination of future CMB and galaxy survey data: Tegmark (1997) has studied a somewhat different and smaller set of the cosmological parameters than we consider here; Hu, Eisenstein, & Tegmark (1997) and Eisenstein, Hu, & Tegmark (1998) have tested the sensitivity of the data to the neutrino mass, which we do not consider in this paper. See also Lineweaver & Barbosa (1998) and Webster et al. (1998), who fit for cosmological parameters using the best available CMB and redshift data available.

Both C_{Tl} and $P_G(k)$ are proportional to the amplitude of the power spectrum of the primordial density fluctuations $A_S^2(k)$. Because of the finite resolution of the MAP satellite, the errors on the C_{Tl} increase rapidly with wavenumber for $l \gtrsim 800$, while the errors on $P_G(k)$ from the SDSS decrease with wavenumber; MAP and SDSS thus quite naturally complement each other in the determination of $A_S^2(k)$. Assuming that inflation occurred, all the obtainable information about the inflationary model is contained in $A_S^2(k)$.

Some inflationary models predict a significant gravity wave contribution to the microwave background fluctuation spectrum at small l . However, even in these models, gravity waves do not make a significant contribution to the microwave background fluctuation spectrum at $l \gtrsim 100$ (Crittenden et al. 1993, Dodelson, Knox, & Kolb 1994, Allen & Koranda 1995, Wang 1996, Turner & Wang 1996). Since most of the information on the cosmological parameters comes from relatively small angular scales ($l \gtrsim 100$), the inclusion of tensor perturbations would not change our results qualitatively.

We parameterize $A_S^2(k)$ by a series of steps equally spaced in $\log k$ bins, each step with a constant amplitude in its bin. By taking these amplitudes to be independent parameters,

we probe features in the primordial power spectrum on all scales. The measurement of the primordial power spectrum independent of specific inflationary models from the combined MAP and SDSS data should shed light on our understanding of the early Universe.

In Section 2, we present the statistical technique we use in estimating errors of parameters. Before considering a general primordial power spectrum, we determine the accuracy with which cosmological parameters will be measured with a pure power law $A_S^2(k)$ in Section 3. In Section 4, we relax this constraint, and discuss the determination of the primordial power spectrum, using the stepwise parameterization described above. Section 5 contains a summary of the paper.

2. The Fisher Information Matrix

The Fisher information matrix of a given set of parameters, \mathbf{s} , approximately quantifies the amount of information on \mathbf{s} that we “expect” to get from our future data. The Fisher matrix can be written as

$$F_{ij} = -\frac{\partial^2 \ln L}{\partial s_i \partial s_j}, \quad (4)$$

where L is the likelihood function, the expected probability distribution of the observables given parameters \mathbf{s} . The Cramér-Rao inequality (Kendall & Stuart 1969) states that no unbiased method can measure the i -th parameter with standard deviation less than $1/\sqrt{F_{ii}}$ if other parameters are known, and less than $\sqrt{(\mathbf{F}^{-1})_{ii}}$ if other parameters are estimated from the data as well. Note that the derivatives in Equation (4) are calculated assuming that the cosmological parameters are given by an a priori model, and thus the errors on the parameters are somewhat dependent on the assumed model.

The likelihood function L in principle can be that of the raw data; see, for example, the discussion in Tegmark et al. (1998) and Dodelson, Hui, & Jaffe (1997). But as Tegmark, Taylor, & Heavens (1997) describe, it is far more convenient to work with the data in a more compressed form. For the galaxy data, we work with the observed galaxy power spectrum, which can be determined using the techniques reviewed, e.g., in Strauss (1997) or Tegmark et al. (1998). The values of the measured power spectrum are approximately statistically independent if measured at values of k spaced at intervals of $2\pi/R$, where R is the characteristic length of the survey volume. Similarly, for a full-sky CMB mapping experiment like MAP, the individual C_l 's are very nearly statistically independent (Oh, Spergel & Hinshaw 1998).

2.1. CMB Data

MAP will measure the CMB polarization as well as temperature anisotropy. The CMB radiation field is described by a 2×2 intensity tensor I_{ij} . The Stokes parameters are $Q \equiv (I_{11} - I_{22})/4$ and $U \equiv I_{12}/2$, while the temperature anisotropy is $\delta T/T \equiv (I_{11} + I_{22})/4$. The temperature anisotropy can be expanded in standard spherical harmonics, while $(Q \pm iU)$ have to be expanded using spin weight ± 2 spherical harmonics ${}_{\pm 2}Y_{lm}$ (Gelfand et al. 1963, Goldberg et al. 1967, Zaldarriaga & Seljak 1997; see also Kamionkowski, Kosowsky, & Stebbins 1997 for an alternative expansion):

$$\begin{aligned} \delta T/T(\hat{\mathbf{n}}) &= \sum_{lm} a_{T,lm} Y_{lm}(\hat{\mathbf{n}}), \\ (Q + iU)(\hat{\mathbf{n}}) &= \sum_{lm} a_{2,lm} {}_2Y_{lm}(\hat{\mathbf{n}}), \\ (Q - iU)(\hat{\mathbf{n}}) &= \sum_{lm} a_{-2,lm} {}_{-2}Y_{lm}(\hat{\mathbf{n}}), \end{aligned} \quad (5)$$

where $\hat{\mathbf{n}}$ is the unit direction vector in the sky. The even and odd parity linear combinations of $a_{2,lm}$ and $a_{-2,lm}$ are

$$\begin{aligned} a_{E,lm} &= -(a_{2,lm} + a_{-2,lm})/2, \\ a_{B,lm} &= i(a_{2,lm} - a_{-2,lm})/2. \end{aligned} \quad (6)$$

Note that $a_{E,lm}$ and $a_{B,lm}$ behave analogously to the electric and magnetic fields respectively under parity transformation. The statistics of the CMB are specified by the power spectra of the variables $(a_{T,lm}, a_{E,lm}, a_{B,lm})$ together with their cross-correlations. For density (scalar) perturbations, the odd parity mode B vanishes. The power spectra can be written as (Seljak & Zaldarriaga 1996)

$$\begin{aligned} C_{Tl} &\equiv \langle |a_{T,lm}|^2 \rangle = (4\pi)^2 \int \frac{dk}{k} A_S^2(k) |\Delta_{Tl}(k, \tau = \tau_0)|^2, \\ C_{El} &\equiv \langle |a_{E,lm}|^2 \rangle = (4\pi)^2 \int \frac{dk}{k} A_S^2(k) |\Delta_{El}(k, \tau = \tau_0)|^2, \\ C_{Cl} &\equiv \langle a_{T,lm}^* a_{E,lm} \rangle = (4\pi)^2 \int \frac{dk}{k} A_S^2(k) \Delta_{Tl}(k, \tau = \tau_0) \Delta_{El}(k, \tau = \tau_0), \end{aligned} \quad (7)$$

where $\Delta_{T,El}(k, \tau = \tau_0)$ are integrals over conformal time τ of the sources which generate the CMB temperature fluctuations and polarization.

The assumption of random-phase density fluctuations does not necessarily imply that the errors on the $C_{T,E,Cl}$ and the $P(k_q)$ are Gaussian-distributed, although the Central Limit Theorem allows us to make this approximation. Following Jungman et al. (1996), Goldberg & Strauss (1998), Tegmark (1997), and Zaldarriaga, Spergel, & Seljak (1997), we can then write the Fisher matrix for the combined MAP and SDSS data as:

$$F_{ij} = \sum_l \sum_{X,Y} \frac{\partial C_{Xl}}{\partial s_i} \text{Cov}^{-1}(C_{Xl}, C_{Yl}) \frac{\partial C_{Yl}}{\partial s_j} + \sum_q \frac{1}{\sigma_{P_q}^2} \frac{\partial P_G(k_q)}{\partial s_i} \frac{\partial P_G(k_q)}{\partial s_j}, \quad (8)$$

where $X, Y = T, E, C$. $\text{Cov}^{-1}(C_{Xl}, C_{Yl})$ is the inverse of the covariance matrix $\text{Cov}(C_{Xl}, C_{Yl}) = \langle \Delta C_{Xl} \Delta C_{Yl} \rangle$. For each l , one has to invert the covariance matrix and sum over X and Y . σ_{P_q} are the standard errors in the measurement of $P(k_q)$ (equation 12 below). We compute the C_{Xl} and $P(k)$ using the CMBFAST Boltzmann code by Uroš Seljak and Matias Zaldarriaga (Seljak & Zaldarriaga 1996). We calculate those derivatives which cannot be found analytically using two-sided finite differences. We take step sizes of 2% of its model value for h , 5% of the model value of Ω_m for Ω_Λ , and 5% of the model value of each parameter for the other parameters.

The covariance matrix of CMB power spectrum estimators has diagonal elements given approximately by (Seljak 1996, Zaldarriaga & Seljak 1997, Kamionkowski, Kosowsky, & Stebbins 1997):

$$\begin{aligned} \text{Cov}(C_{Tl}^2) &= \frac{2}{(2l+1)f_{sky}} \left(C_{Tl} + w_T^{-1} B_l^{-2} \right)^2, \\ \text{Cov}(C_{El}^2) &= \frac{2}{(2l+1)f_{sky}} \left(C_{El} + w_P^{-1} B_l^{-2} \right)^2, \\ \text{Cov}(C_{Cl}^2) &= \frac{1}{(2l+1)f_{sky}} \left[C_{Cl}^2 + \left(C_{Tl} + w_T^{-1} B_l^{-2} \right) \left(C_{El} + w_P^{-1} B_l^{-2} \right) \right], \end{aligned} \quad (9)$$

while the off-diagonal matrix elements are:

$$\begin{aligned} \text{Cov}(C_{Tl} C_{El}) &= \frac{2}{(2l+1)f_{sky}} C_{Cl}^2, \\ \text{Cov}(C_{Tl} C_{Cl}) &= \frac{2}{(2l+1)f_{sky}} C_{Cl} \left(C_{Tl} + w_T^{-1} B_l^{-2} \right), \\ \text{Cov}(C_{El} C_{Cl}) &= \frac{2}{(2l+1)f_{sky}} C_{Cl} \left(C_{El} + w_P^{-1} B_l^{-2} \right), \end{aligned} \quad (10)$$

where f_{sky} is the fraction of sky which is mapped. We take $f_{sky} = 0.8$ for MAP. We have defined $w_{(T,P)}^{-1} \equiv \sigma_{(T,P)}^2 \theta_{fwhm,c}^2$, where $\sigma_{T,P}$ is the noise per pixel in the temperature and the polarization measurements, and θ_{fwhm} is the full width at half maximum of the beam in radians. The quantity $B_l^2 \equiv \exp \left[- (0.425 \theta_{fwhm} l)^2 \right]$ is the window function of the Gaussian beam.

For MAP, both temperature and polarization data are obtained from the same experiment by adding and differencing the two polarization states, hence $\sigma_T^2 = \sigma_P^2/2$, and the noise and polarization signals are uncorrelated. MAP's resolution at its three highest frequency channels (40, 60, and 90 GHz) is anticipated to be $\theta_{fwhm} = 0.47^\circ$, 0.35° , and 0.21° respectively, with the corresponding $\sigma_T = 27 \mu\text{K}$, $35 \mu\text{K}$, and $35 \mu\text{K}$ for its two year nominal mission (Bennett et al. 1997; <http://map.gsfc.nasa.gov>). We do a weighted average in the three channels c , yielding

$$w_T = \sum_c w_T^c = \sum_c \frac{1}{\sigma_{T,c}^2 \theta_{fwhm,c}^2} = \frac{1}{(0.10 \mu\text{K})^2},$$

$$\begin{aligned}
 w_P &= w_T/2, \\
 B_l^2 &= \frac{\sum_c w_T^c B_{l,c}^2}{\sum_c w_T^c} = \frac{\sum_c e^{-l^2 \sigma_{b,c}^2} / (\sigma_{T,c}^2 \theta_{fwhm,c}^2)}{\sum_c 1 / (\sigma_{T,c}^2 \theta_{fwhm,c}^2)}.
 \end{aligned}
 \tag{11}$$

In our analysis, we ignore foreground contamination. Current estimates (Efstathiou & Bond 1998; Refregier et al. 1998) suggest that foregrounds will not significantly affect MAP temperature data. Foreground contamination, however, may significantly limit analyses of polarization data, particularly at low l (Keating et al. 1998). Thus, we report our results both for analyses that use only the temperature data and for analyses that use both the temperature and polarization data.

2.2. Galaxy Data

We take the SDSS standard error in the measured galaxy power spectrum from Feldman, Kaiser, & Peacock (1994). For the power spectrum determined over a volume in k -space of V_k :

$$\frac{\sigma_P}{P_G(k)} = \left(\frac{(2\pi)^3 \int d^3\mathbf{r} \bar{n}^4(\mathbf{r}) \psi^4(\mathbf{r}) \left[1 + \frac{1}{\bar{n}(\mathbf{r}) P_G(k)}\right]^2}{V_k [\int d^3\mathbf{r} \bar{n}^2(\mathbf{r}) \psi^2(\mathbf{r})]^2} \right)^{1/2},
 \tag{12}$$

where $\bar{n}(\mathbf{r})$ is the selection function, and $\psi(\mathbf{r})$ is the weighting function. For spherical shells, $V_{k_q} = \frac{4}{3}\pi(k_q^3 - k_{q-1}^3)$, where again, the spacing between the k_q is $2\pi/R$. We choose $R = 1466 h^{-1} \text{Mpc}$ for the SDSS, following Goldberg & Strauss (1998). We use the SDSS selection function calculated by Goldberg & Strauss (1998) using a mock SDSS redshift sample created by D. Weinberg (cf., Cole et al. 1998). We take the weighting function $\psi(\mathbf{r}) = 1$ throughout. Equation (12) assumes that the power estimates in each k band are uncorrelated. Goldberg & Strauss (1998) show that this assumption causes at most a 10% underestimation of the true errors of parameters.

3. Determination of the Cosmological Parameters

In this section, we discuss how well the cosmological parameters can be determined by combining the MAP and SDSS data. Although we consider a general primordial power spectrum in Sec. 4, we here restrict ourselves to the simpler case of a power-law model for the primordial power spectrum generated by inflation, $k A_S^2(k) \propto k^{n_S}$. We consider h , Ω_Λ , Ω_b , τ_{ri} , n_S , Ω_m , $C_2 \equiv |a_{T,2m}|^2$ (which sets the CMB normalization), and b_{eff} as free parameters. In Sec. 4, we will see how our determination of these quantities worsens once we give up a priori constraints on $A_S^2(k)$.

The Fisher matrix depends on the true underlying power spectrum. We consider here

three models, standard cold dark matter model (SCDM), the CDM model with cosmological constant (Λ CDM), and open CDM (OCDM). The model values of the cosmological parameters are shown in Table 1. The C_2 values in Table 1 are obtained by normalizing the models to the COBE four-year data, following Bunn & White (1997). We take the galaxy bias parameter to be $b = 1/\sigma_8$, with σ_8 derived using the model C_2 value, and using the standard value for the observed fluctuations of galaxies within $8 h^{-1}\text{Mpc}$ spheres (Davis & Peebles 1983). Note that as we vary parameters to compute the Fisher matrix, we keep $\Omega_m + \Omega_\Lambda = 1$ for the SCDM and Λ CDM models, because these models are flat by definition. In the open CDM model, we allow for the simultaneous determination of Ω_m and Ω_Λ .

Table 1: Model values of cosmological parameters

	h	Ω_Λ	Ω_b	τ_{ri}	n_S	Ω_m	C_2	$b = 1/\sigma_8$
SCDM	0.5	0	0.05	0.05	1	1	1.139×10^{-10}	0.83
Λ CDM	0.65	0.7	0.06	0.1	1	0.3	1.455×10^{-10}	1.29
OCDM	0.65	0	0.06	0.05	1	0.4	1.607×10^{-10}	1.72

In the linear theory of mass density fluctuations, the bias factor b is degenerate with the CMB normalization C_2 . Nonlinear effects in the present-day galaxy power spectrum break this degeneracy. We include nonlinear effects following Peacock & Dodds (1996). Given a linear power spectrum $P_L(k_L)$, the effective local power law index can be defined as

$$n_{eff}(k_L) = n_L(k_L) = \left. \frac{d \ln P_L}{d \ln k} \right|_{k=k_L/2}. \quad (13)$$

The nonlinear power spectrum $P_{NL}(k)$ is related to the linear power spectrum by

$$\Delta_{NL}^2(k_{NL}) = f_{NL}(\Delta_L^2(k_L), \Omega), \quad (14)$$

where $\Delta_L^2(k_L) \equiv k_L^3 P_L(k_L)/(2\pi^2)$, and $\Delta_{NL}^2 \equiv k^3 P_{NL}(k)/(2\pi^2)$.

$$f_{NL}(x, \Omega) = x \left[\frac{1 + B\gamma x + [Ax]^{\alpha\gamma}}{1 + ([Ax]^\alpha g^3(\Omega)/[Vx^{1/2}])^\gamma} \right]^{1/\gamma} \quad (15)$$

with

$$\begin{aligned} A &= 0.482 (1 + n_{eff}/3)^{-0.947}, \\ B &= 0.226 (1 + n_{eff}/3)^{-1.778}, \\ \alpha &= 3.310 (1 + n_{eff}/3)^{-0.244}, \\ \gamma &= 0.862 (1 + n_{eff}/3)^{-0.287}, \\ V &= 11.55 (1 + n_{eff}/3)^{-0.423}, \end{aligned} \quad (16)$$

and (Carroll, Press, & Turner 1992)

$$g(\Omega) = \frac{5}{2} \Omega_m \left[\Omega_m^{4/7} - \Omega_\Lambda + (1 + \Omega_m/2)(1 + \Omega_\Lambda/70) \right]^{-1}. \quad (17)$$

The nonlinear wavenumber is related to the linear wavenumber by

$$k_{NL} = k_L [1 + \Delta_{NL}^2(k_{NL})]^{1/3}. \quad (18)$$

Note that although our consideration of nonlinear effects is adequate in the context of this paper, it is inaccurate in several ways. First, even though we include nonlinear effects in $P(k)$, we still use Kaiser’s linear relation for redshift effects. Proper consideration of redshift distortions on small scales (Fisher & Nusser 1996, Hatton & Cole 1998) will lead to an effective bias b_{eff} which depends on k as well as the cosmological parameters b and Ω_m . Second, we have explicitly assumed that the true bias b in real space is exactly linear and constant with scale; there must be scale-dependence and non-linearities, especially at small scales, where the density fluctuations are large (cf., Dekel & Lahav 1998; Blanton et al. 1998). Third, as the strength of the baryon-induced wiggles in the power spectrum is proportional to Ω_b/Ω_m , they are more pronounced in the Λ CDM and OCDM models. The Peacock & Dodds (1996) non-linear formulae only apply to *smooth* linear power spectra; we therefore smooth the linear power spectra of the Λ CDM and OCDM models (using the analytical formulae in Eisenstein & Hu 1998) before applying the non-linear formulae. Since we are discarding the information contained in the baryon-induced wiggles, we obtain overestimates of the true errors. Finally, non-linear effects will cause mode-mixing between estimates of the power spectrum we have assumed here to be independent (cf., Jain & Bertschinger 1994). These effects are difficult to include in the Fisher matrix formalism, and we do not attempt to do so here. We carry out all calculations in this section to two limits in the k_q of the galaxy power spectrum, $k_{max} = 0.1 h \text{ Mpc}^{-1}$ and $k_{max} = 0.5 h \text{ Mpc}^{-1}$. The Peacock & Dodds (1996) formalism indicates that for the models considered here, non-linear effects become significant for values of k somewhat larger than $0.1 h \text{ Mpc}^{-1}$. So the former value of k_{max} corresponds to a scale where non-linear effects are negligible, while the latter corresponds to a scale $2\pi/k \approx 12 h^{-1} \text{ Mpc}$ where nonlinear effects are becoming strong. It is work for the future to check the validity of our calculations in this non-linear regime.

To calculate the Fisher matrix, we need the derivatives of the C_{Xl} ’s (X denotes T , E , C) and $P_G(k) = b_{eff}^2 P_{NL}(k)$ with respect to the cosmological parameters. The derivatives with respect to C_2 and b_{eff} can be found analytically:

$$\begin{aligned} \frac{\partial C_{Xl}}{\partial \ln C_2} &= C_{Xl}, \\ \frac{\partial C_{Xl}}{\partial \ln b_{eff}} &= 0, \\ \frac{\partial P_G(k)}{\partial \ln C_2} &= P_G(k) \frac{\partial \ln f_{NL}(x, \Omega)}{\partial \ln x}, \end{aligned}$$

$$\frac{\partial P_G(k)}{\partial \ln b_{\text{eff}}} = 2 P_G(k), \quad (19)$$

where $x \equiv \Delta_L^2(k_L)$, and k_L is related to k via equation (18). In the OCDM model, we take both Ω_Λ and Ω_m to be free parameters. Hence

$$\frac{\partial P_G(k)}{\partial \Omega_\Lambda} = P_G(k) \left[\left. \frac{\partial \ln f_{NL}(x, \Omega)}{\partial \Omega_\Lambda} \right|_x + \left. \frac{\partial \ln f_{NL}(x, \Omega)}{\partial \ln x} \right|_{\Omega_\Lambda} \cdot \frac{\partial \ln P_L(k_L)}{\partial \Omega_\Lambda} \right], \quad (20)$$

where $P_L(k_L)$ depends on Ω_Λ only through an overall normalization for the k range relevant to redshift surveys (on superhorizon scales, $P_L(k_L)$ has a k -dependent Ω_Λ dependence in the OCDM model). The derivatives with respect to the other cosmological parameters are calculated numerically by finite differences.

Tables 2, 3, and 4 show the Fisher Matrix $1\text{-}\sigma$ error bars for the cosmological parameters, $\Delta s_i = \sqrt{(\mathbf{F}^{-1})_{ii}}$ for SCDM, Λ CDM, and OCDM respectively. For each parameter, we list the errors for six cases: the MAP temperature data taken alone, the MAP temperature data with SDSS data to $k_{\text{max}} = 0.1 \text{ hMpc}^{-1}$, the MAP temperature data with SDSS data to $k_{\text{max}} = 0.5 \text{ hMpc}^{-1}$, and the corresponding results when MAP polarization data are included as well.

Table 2: Fisher Matrix $1\text{-}\sigma$ error bars for the cosmological parameters of SCDM.

$1\text{-}\sigma$ error	MAP ^T	MAP ^T + SDSS ¹	MAP ^T + SDSS ²	MAP ^(T+P)	MAP ^(T+P) + SDSS ¹	MAP ^(T+P) + SDSS ²
$\Delta \ln C_2$	0.17	0.097	0.016	0.065	0.053	0.016
$\Delta \ln h$	0.052	0.041	0.021	0.033	0.028	0.018
$\Delta \Omega_\Lambda$	0.15	0.11	0.057	0.091	0.076	0.047
$\Delta \ln(\Omega_b h^2)$	0.028	0.024	0.019	0.020	0.019	0.017
$\Delta \ln \tau_{ri}$	2.4	1.5	0.46	0.39	0.38	0.30
$\Delta \ln n_S$	0.017	0.014	0.0081	0.0085	0.0076	0.0059
$\Delta \ln b_{\text{eff}}$		0.064	0.028		0.063	0.022

Note. — “T” denotes temperature only, “(T+P)” denotes temperature plus polarization for MAP data. “1” and “2” denote the SDSS cutoff $k_{\text{max}} = 0.1 \text{ hMpc}^{-1}$, and 0.5 hMpc^{-1} respectively.

The peak features (called “Doppler peaks”, “acoustic peaks”, or “Sakharov peaks”) in the CMB angular power spectrum $C_{\ell l}$ are due to acoustic oscillations in the baryon-photon

Table 3: Fisher Matrix 1- σ error bars for the cosmological parameters of Λ CDM.

1- σ error	MAP ^T	MAP ^T + SDSS ¹	MAP ^T + SDSS ²	MAP ^(T+P)	MAP ^(T+P) + SDSS ¹	MAP ^(T+P) + SDSS ²
$\Delta \ln C_2$	0.21	0.15	0.010	0.043	0.043	0.010
$\Delta \ln h$	0.066	0.048	0.025	0.032	0.030	0.021
$\Delta \ln \Omega_\Lambda$	0.076	0.055	0.027	0.037	0.035	0.023
$\Delta \ln(\Omega_b h^2)$	0.044	0.034	0.022	0.021	0.021	0.018
$\Delta \ln \tau_{ri}$	1.33	0.95	0.18	0.18	0.18	0.13
$\Delta \ln n_S$	0.035	0.026	0.014	0.014	0.013	0.011
$\Delta \ln b_{eff}$		0.076	0.022		0.038	0.021

Table 4: Fisher Matrix 1- σ error bars for the cosmological parameters of OCDM.

1- σ error	MAP ^T	MAP ^T + SDSS ¹	MAP ^T + SDSS ²	MAP ^(T+P)	MAP ^(T+P) + SDSS ¹	MAP ^(T+P) + SDSS ²
$\Delta \ln C_2$	0.13	0.10	0.034	0.081	0.064	0.033
$\Delta \ln h$	0.11	0.085	0.018	0.093	0.069	0.015
$\Delta \ln \Omega_m$	0.13	0.099	0.011	0.13	0.083	0.010
$\Delta \Omega_\Lambda$	0.088	0.060	0.010	0.085	0.055	0.0097
$\Delta \ln(\Omega_b h^2)$	0.041	0.033	0.017	0.038	0.031	0.017
$\Delta \ln \tau_{ri}$	1.5	1.5	0.46	0.57	0.57	0.37
$\Delta \ln n_S$	0.026	0.021	0.0079	0.023	0.020	0.0076
$\Delta \ln b_{eff}$		0.14	0.029		0.14	0.026

fluid at the time of last scattering of the CMB photons. As mentioned above, the amplitude of these peaks is determined by $\Omega_b h^2$ and $\Omega_m h^2$, while their location is determined by the geometry of the universe (roughly $\Omega_m + \Omega_\Lambda$ in a nearly flat universe), hence there is a near degeneracy in one dimension of the parameter space of h , Ω_b , Ω_Λ and Ω_m (Bond et al. 1994; Zaldarriaga, Spergel & Seljak 1997; Huey & Dave 1997). For models with only six or seven free parameters, this degeneracy is not severe (see Table 2); however, it is significant if we consider models with many more free parameters (e.g., a variable spectral index, or massive neutrinos).

Large scale structure observations are sensitive to an orthogonal set of parameters. The turnover in the matter power spectrum is set by the horizon size at matter-radiation equality (e.g., Peebles 1993). Thus, SDSS will make an accurate measurement of $\Omega_m h$.

The Silk damping scale, and the acoustic oscillations also affect the transfer function, so that $\Omega_b h$ can also be determined from the SDSS observations (Goldberg & Strauss 1998). Thus combining the MAP and SDSS data allows us to do two important things. First, to the extent that parameters derived from the two independent data sets are consistent, we obtain a powerful check of the correctness of the physical model which ties the two together: gravitational instability theory, the assumption that the fluctuations are adiabatic, and the linear biasing paradigm. This is illustrated in Figure 1, which shows the 68.3% and 95.4% confidence contours in the Ω_b - h (a) and Ω_m - h (b) planes. The dotted lines are for MAP temperature data only, the dashed lines are for SDSS data only ($k_{max} = 0.5 h\text{Mpc}^{-1}$), and the solid lines are for the combined MAP temperature and SDSS data. The SCDM model is assumed. Second, the joint analysis of the two independent data sets breaks some of the degeneracies inherent in the MAP data taken alone and improves the accuracy in the determination of parameters. Figure 2 shows the 68.3% and 95.4% confidence contours in the Ω_Λ - Ω_m plane in the Λ CDM model, with the same line types as in Figure 1. Note that using MAP data alone, there is degeneracy between Ω_m and Ω_Λ ; using SDSS data alone, Ω_Λ can not be determined because it is degenerate with C_2 (see equation 20). The combined data give a much better determination of Ω_m and Ω_Λ than does either the MAP data or the SDSS data alone.

The CMB temperature spectrum is also approximately degenerate in its dependence on the reionization optical depth τ_{ri} and the CMB normalization C_2 , because reionization suppresses the spectrum by a factor of $\exp(-2\tau_{ri})$ on small scales relative to the large scales. Figure 3 shows the confidence contours in the τ_{ri} - C_2 plane, with the same line types as in Figure 1. Combining MAP data with SDSS data dramatically breaks the degeneracy between τ_{ri} and C_2 by adding information on the small scales.

Figures 1-3 show MAP temperature data only, because the extent to which MAP polarization data can be used may be limited by foregrounds (see Section 5). Also, if we allow a cutoff of $k_{max} = 0.5 h\text{Mpc}^{-1}$ (as we do for the rest of this paper), adding MAP polarization data to the combined MAP and SDSS data does not have a significant impact on the accuracy of the determination of cosmological parameters (see Tables 2-4).

Note that the errors of the parameters from combined MAP and SDSS data are very sensitive to the SDSS cutoff k_{max} . This is as expected, since the small scale information from the SDSS is determined by its cutoff k_{max} . Indeed, in most cases, the galaxy data to $k_{max} = 0.1 h\text{Mpc}^{-1}$ gives only a moderate improvement to the constraints the MAP data alone give; much of the improvement comes from the non-linear galaxy regime.

To summarize, when MAP temperature data is considered alone, there is strong degeneracy between the overall amplitude of the matter power spectrum C_2 and the reionization optical depth τ_{ri} , and between the matter density fraction Ω_m and the density fraction contribution from cosmological constant Ω_Λ . Combining MAP and SDSS data dramatically breaks the degeneracy between C_2 and τ_{ri} , and reduces the degeneracy

between Ω_m and Ω_Λ , leading to a significant improvement on the determination of C_2 , τ_{ri} , Ω_m , and Ω_Λ , enabling us to measure the effective bias between the matter power spectrum and the galaxy redshift power spectrum b_{eff} . The accuracy in the determination of other cosmological parameters is also improved by combining MAP and SDSS data, but to a less impressive extent. In the next section, we study the measurement of the primordial power spectrum itself, which can only be achieved by using the combined MAP and SDSS data.

4. Measurement of the Primordial Power Spectrum

In the previous section, we considered a power-law primordial power spectrum, and derived the constraints on cosmological models that the combination of MAP and SDSS data will give. We now consider a more general primordial power spectrum; as we discussed in the Introduction, various inflationary models make a range of predictions for the form of the primordial power spectrum. We parameterize the primordial power spectrum $A_S^2(k)$ as

$$A_S^2(k) = \begin{cases} a_1, & \text{for } k < k_1, \\ a_i, & \text{for } k_{i-1} < k < k_i, \quad i > 1 \end{cases} \quad (21)$$

where $k_1 = 0.001 h\text{Mpc}^{-1}$, and k_i ($i = 2, 3, \dots, 20$) are equally spaced in $\log k$ from k_1 to $k = 0.5 h\text{Mpc}^{-1}$. The a_i ($i = 1, 2, \dots, 20$) are taken to be independent variables. To compute errors in the determination of the a_i , we need to know their true values, as well as true values of the cosmological parameters. We first consider the case that the cosmological parameters are known a priori; we consider the realistic case in which we know neither the primordial power spectrum nor the cosmological parameters later in this section. For definiteness, we adopt a model in which the true primordial power spectrum is $A_S^2(k) = 1$, and the cosmological parameters are those of ΛCDM (see Table 1).

In the Fisher matrix approach we have adopted in this paper, we need to compute the derivatives of the observables with respect to the parameters, which now include the values of the steps a_i which make up the primordial power spectrum. The derivatives of the C_l 's with respect to a_i are taken to be finite differences with step-size of 5% the model value of a_i . The derivatives of the galaxy power spectrum with respect to a_i are given by

$$\frac{\partial \ln P_G(k)}{\partial a_i} = \begin{cases} \frac{\partial \ln f_{NL}(x)}{\partial \ln x} \frac{1}{a_i}, & \text{for } k < k_1 \quad (i = 1), \text{ or } k_{i-1} < k < k_i \quad (i > 1), \\ 0, & \text{otherwise,} \end{cases} \quad (22)$$

where x and $f_{NL}(x)$ are the same as in Equation (19).

In this section, we take the cutoff wavenumber of the SDSS to be $k = 0.5\text{Mpc}^{-1}$ throughout. Also, when we consider the combined MAP and SDSS data, only the temperature data from MAP is used; adding the polarization data does not have a significant effect on errors from the combined MAP and SDSS data, while it is of great

interest to consider the SDSS data as an *alternative* to the MAP polarization data in constraining inflationary models.

Figure 4 shows the accuracy in the determination of the bin amplitudes of the primordial power spectrum, $k A_S^2(k)$; the $1\text{-}\sigma$ error bars are shown for MAP temperature data only (a), SDSS data only (b), and MAP temperature and SDSS data combined (c). Assuming the cosmological parameters are known, for 20 bins in $\log k$ ($k \leq 0.5 h \text{Mpc}^{-1}$), the primordial power spectrum can be determined to around 16% accuracy for $k \sim 0.01 h \text{Mpc}^{-1}$, and to around 1% accuracy for $k \sim 0.1 h \text{Mpc}^{-1}$ (see Figure 4(c)) by combining MAP temperature and SDSS data.

Not surprisingly, the determination of the primordial power spectrum bin amplitudes does depend on the a priori knowledge of the cosmological parameters. We now consider the realistic case in which the cosmological parameters are not known a priori; in particular, in addition to the a_i , we also solve for the four parameters h , Ω_Λ , Ω_b , and τ_{ri} . The primordial power spectrum bin amplitudes and the cosmological parameters can not be simultaneously determined using MAP temperature data only, because τ_{ri} is degenerate with the a_i for $k \gtrsim 0.01 h \text{Mpc}^{-1}$. However, polarization data removes this degeneracy. Figure 5(a) shows the resulting error bars on the a_i if both the temperature and polarization data from MAP are used; they are significantly larger than in Figure 4(a) where only temperature data is used.

Figure 5(b) shows the effect of combining the MAP temperature data with the SDSS data in the analysis, adding the galaxy bias b_{eff} as a fifth parameter. The uncertainty in the determination of the primordial power spectrum bin amplitudes a_i increases by a factor up to 3 on small scales relative to the case in which the cosmological parameters are known a priori (Figure 4(c)). This difference is indistinguishable in the figures, because it enters through error bars that are only of the order of a few percent. The errors in the a_i are not significantly increased by the inclusion of cosmological parameters in the parameter estimation, because most of the information on the cosmological parameters comes from small angular scales, where the power spectrum can be determined to great accuracy from the SDSS data. Comparison of Figure 5(a) and Figure 5(b) illustrates the critical importance of combining the MAP data with the SDSS data in the determination of the primordial power spectrum bin amplitudes.

Note that our choice of 20 bins in $\log k$ to parameterize $A_S^2(k)$ is somewhat arbitrary. Obviously, the errors on the bin amplitudes would increase if we were to increase the number of bins. When the cosmological parameters are estimated together with the $A_S^2(k)$ bin amplitudes a_i , we expect the covariance between the cosmological parameters and the a_i 's to increase rapidly with smaller bin size, as the primordial power spectrum becomes flexible enough to mimic the Doppler peaks and other features of the C_l .

To illustrate how the errors on the cosmological parameters change as they are estimated jointly with primordial power spectrum bin amplitudes using the combined MAP

temperature and SDSS data, we show in Table 5 the Fisher matrix $1\text{-}\sigma$ error bars for two groups of cosmological parameters, $(h, \Omega_b, \tau_{ri}, b_{eff})$ and $(h, \Omega_\Lambda, \Omega_b, \tau_{ri}, b_{eff})$, when they are estimated jointly within each group and when each group is simultaneously estimated with 20 independent bin amplitudes of the primordial power spectrum. The cosmological

Table 5: Fisher Matrix $1\text{-}\sigma$ error bars for the cosmological parameters.

$1\text{-}\sigma$ error	4 parameters	4 parameters & 20 bin amplitudes of $A_S^2(k)$	5 parameters	5 parameters & 20 bin amplitudes of $A_S^2(k)$
$\Delta \ln h$	0.0048	0.0062	0.017	0.025
$\Delta \Omega_\Lambda$			0.046	0.064
$\Delta \ln(\Omega_b h^2)$	0.016	0.039	0.016	0.046
$\Delta \ln \tau_{ri}$	0.056	0.19	0.12	0.27
$\Delta \ln b_{eff}$	0.0052	0.0094	0.012	0.017

parameters can still be determined to impressive accuracy even when they are estimated simultaneously with 20 independent bin amplitudes of the primordial power spectrum! Of course, we do not include the overall amplitude of the power spectrum C_2 as a free parameter, as it is degenerate with the a_i by definition.

Figures 4 and 5 assume that the true primordial power spectrum is $A_S^2(k) = 1$. For the purpose of illustration, we can choose our model primordial power spectrum $A_S^2(k)$ to have broken scale-invariance based on the Holman et al. (1991) and Adams et al. (1997) models. We write

$$A_S^2(k) = \begin{cases} 1, & k < 0.01 \text{ hMpc}^{-1}, \\ A + Bk, & 0.01 \text{ hMpc}^{-1} < k < 0.1 \text{ hMpc}^{-1}, \\ 0.25 k^{-0.2}, & k > 0.1 \text{ hMpc}^{-1}, \end{cases} \quad (23)$$

where A and B are chosen such that $A_S^2(k)$ is continuous. Figure 6 shows the primordial power spectrum of Equation (23) with $1\text{-}\sigma$ error bars for the combined MAP temperature and SDSS data. Clearly, the accuracy in the determination of $A_S^2(k)$ is not sensitive to the assumed underlying model; the errors on $A_S^2(k)$ bin amplitudes do not change significantly with model where the errors are larger than of order a few percent.

There have been recent claims of possible observational detection of features in the matter power spectrum on the scale of $k \sim 0.1 \text{ hMpc}^{-1}$ (Peacock 1997). Combining MAP and SDSS data will enable us to confirm such features, and to determine whether they are intrinsic to the primordial power spectrum, independent of specific inflationary models. Indeed, it would be straightforward to translate our bin amplitude errors of the primordial power spectrum into constraints on existing inflationary models; our errors are small enough to be very interesting. However, it is perhaps more exciting to anticipate that the

measurement of the primordial power spectrum in wavenumber bins from the combined MAP and SDSS data will provide a lead to the correct inflationary model.

5. Summary

Cosmic microwave background experiments measure fluctuations in the curvature of space at the surface of last scattering. If the primordial fluctuations are adiabatic, then MAP will be a sensitive probe of the geometry of the universe, the matter/photon ratio ($\Omega_m h^2$), the baryon/photon ratio ($\Omega_b h^2$) and the primordial power spectrum for $k < 0.2 h\text{Mpc}^{-1}$.

Observations of large scale structure measure the large scale distribution of galaxies. If the primordial fluctuations are adiabatic, then SDSS will be a sensitive probe of the primordial power spectrum for $k > 0.02 h\text{Mpc}^{-1}$ and $\Omega_m h$, which determines the horizon size at matter-radiation equality and thus the shape of the processed power spectrum. SDSS will also be a powerful probe of the nature of the dark matter (Hu et al. 1997). Because of the large number of galaxies with detailed photometric and spectroscopic data in the SDSS, we can determine the power spectrum and bias factor for several independent samples of galaxies, defined by morphology, color, or spectral characteristics. To the extent to which these independent samples yield consistent power spectra, we can determine the range in k over which the linear bias model is valid.

The combination of the SDSS and the MAP data will be a powerful test of our basic cosmological models. Both experiments will accurately determine the amplitude of density fluctuations at $0.2 > k > 0.02 h\text{Mpc}^{-1}$. Will there be a set of cosmological parameters and primordial power spectrum that is consistent with both sets of observations? If so, then we will have tested the gravitational structure formation paradigm, our interpretation of the primordial fluctuations as adiabatic, and the linear biasing paradigm. If not, this conflict will likely lead us to a deeper understanding of the origin of structure in the universe.

In particular, from the combination of the MAP and SDSS data, we can obtain a measurement of the primordial power spectrum without reference to any specific inflationary model, assuming that the primordial fluctuations are adiabatic. If the values of the cosmological parameters that best fit the data are close to what we expect, but the primordial power spectrum differs significantly from the predictions of the current inflationary models, then it will be an indication of new physics in the early universe, and it will provide a solid starting point for building new inflationary models.

If there is a theory consistent with both data sets, then the combination of the two observations will break the degeneracies inherent in each individual observation. Cosmic microwave background observations by themselves measure a combination of the amplitude of the primordial power spectrum and the optical depth. Large scale structure observations

measure the product of the current matter power spectrum and the bias parameter. In linear theory, the offset between the power spectrum as determined by the two sets of observations determines a combination of the bias parameter and the optical depth of the universe. Because of non-linear effects on the spectrum, this offset is scale-dependent, this will enable us to independently measure the bias parameter and the optical depth of the universe. The combination of the two experiments will also improve our ability to determine other cosmological parameters, in particular, the matter density and the cosmological constant.

Measurements of the cosmic microwave background polarization can provide an independent measure of the optical depth of the universe τ_{ri} (Zaldarriaga, Spergel & Seljak 1997). However, emission from both polarized galactic dust and synchrotron emission (Keating et al. 1998) may swamp the primordial polarization fluctuations at large angular scales. These foregrounds may significantly limit our ability to extract useful cosmological information from polarization measurements. Hence it is important that we can use the SDSS data as an alternative and independent aid to MAP in the determination of τ_{ri} .

The Sloan Digital Sky Survey, and other large scale structure surveys, will make other independent measurements that will probe cosmological parameters and the primordial spectrum: redshift distortions, cluster properties, small scale velocity fields, and the evolution of structure. These will provide additional tests of the basic model and will further enhance our ability to measure cosmological parameters.

With this in mind, there are a number of improvements that could be done in this analysis. The redshift distortions could be measured directly, and the effects could be included directly into the Fisher matrix analysis (cf., de Laix & Starkman 1998 and Hatton & Cole 1998 for a discussion of how well redshift-space distortions can be measured from the SDSS data). Similarly, we could parameterize the effects of galaxy and clustering evolution, and include these as parameters in the analysis. More challenging will be a proper accounting of non-linear effects on small scales, in the power spectrum, the redshift space distortions, and the bias (here assumed linear and independent of scale). The analyses in Tables 2-4 show that going to $k_{max} = 0.5 h\text{Mpc}^{-1}$ gives us particularly strong constraints on cosmological parameters, but we have taken the non-linear effects into account in only a relatively crude way in this paper. It remains to be seen the extent to which the uncertainties due to these inaccuracies strongly affect the error bars we derive on the primordial power spectrum.

The next few years will be a very exciting time in cosmology.

6. Acknowledgements

Y.W. acknowledges partial support from NSF grant AST94-19400. DNS acknowledges support from the MAP/MIDEX project. MAS acknowledges support from the Alfred P. Sloan Foundation, a fellowship from Research Corporation, and NSF grant AST96-16901. We acknowledge the use of CMBFAST Boltzmann code by Uroš Seljak and Matias Zaldarriaga. It is a pleasure for us to thank Matias Zaldarriaga for many helpful clarifications concerning CMBFAST, and Daniel Eisenstein and Wayne Hu for emphasizing the importance of two-sided derivatives.

REFERENCES

- Adams, J.A., Ross, G.G., & Sarkar, S. 1997, *Nuclear Physics B*, 503, 405
- Allen, B., & Koranda, S. 1995, *Phys. Rev. D*, 52, 1902
- Bennett, C.L., Halpern, M., Hinshaw, G., Jarosik, N., Limon, M., Mather, J., Meyer, S.S., Page, L., Spergel, D.N., Tucker, G., Wilkinson, D.T., Wollack, E. & Wright, E.L. 1997, *BAAS*, 29, 1353
- Blanton, M., Cen, R., Ostriker, J.P., & Strauss, M.A. 1998, submitted to *ApJ* (astro-ph/9807029)
- Bond, J. R., Crittenden, R., Davis, R.L., Efstathiou, G., & Steinhardt, P.J. 1994, *Phys. Rev. Lett.*, 72, 13
- Bond, J.R., Efstathiou, G., & Tegmark, M. 1997, *MNRAS*, 291, L33
- Bunn, E.F. & White, M. 1997, *ApJ*, 480, 6
- Carroll, S.M., Press, W.H., & Turner, E.L. 1992, *ARA&A*, 30, 499
- Cole, S., Hatton, S., Weinberg, D.H., & Frenk, C.S. 1998, preprint (astro-ph/9801250)
- Copeland, E.J., Grivell, I.J., & Liddle, A.R. 1997, preprint (astro-ph/9712028)
- Crittenden, R., Bond, J.R., Davis, R.L., Efstathiou, G., & Steinhardt, P.J. 1993, *Phys. Rev. Lett.*, 71, 324
- Davis, M., & Peebles, P.J.E. 1983, *ApJ*, 267, 465
- Dekel, A., & Lahav, O. 1998, preprint (astro-ph/9806193)
- de Laix, A.A., & Starkman, G. 1998, *ApJ*, 501, 427
- Dodelson, S., Hui, L., & Jaffe, A. 1997, preprint (astro-ph/9712074)
- Dodelson, S., Kinney, W.H., & Kolb, E.W. 1997, *Phys. Rev. D*, 56, 3207
- Dodelson, S., Knox, L., & Kolb, E.W. 1994, *Phys. Rev. Lett.* 72, 3444
- Efstathiou, G. & Bond, J.R. 1998, preprint (astro-ph/9807103)
- Eisenstein, D.J. & Hu, W. 1998, *ApJ*, 496, 605
- Eisenstein, D.J., Hu, W., & Tegmark, M. 1998, preprint (astro-ph/9807130)
- Feldman, H.A., Kaiser, N., & Peacock, J.A. 1994, *ApJ*, 426, 23

- Fisher, K.B., & Nusser, A. 1996, MNRAS, 279, L1
- Freese, K., Frieman, J.A., & Olinto, A.V. 1990, Phys. Rev. Lett., 65, 3233
- Fry, J.N., & Wang, Y. 1992, Phys. Rev., D46, 3318
- Gelfand, I.M., Minlos, R.A., & Shapiro, Z. Ya. 1963, Representations of the Rotation and Lorentz Groups and Their Applications (Pergamon:Oxford)
- Goldberg, J.N., et al. 1967, J. Math. Phys., 8, 2155
- Goldberg, D.M., & Strauss, M.A. 1998, ApJ, 495, 29
- Gunn, J. E., & Weinberg, D. H. 1995, in *Wide-Field Spectroscopy and the Distant Universe*, ed. S. J. Maddox and A. Aragón-Salamanca (Singapore: World Scientific), 3
- Hamilton, A.J.S. 1998, in *Ringberg Workshop on Large-Scale Structure*, ed. D. Hamilton (Kluwer, Amsterdam)
- Hatton, S.J., & Cole, S. 1998, MNRAS, 296, 10
- Holman, R., Kolb, E.W., Vadas, S.L., & Wang, Y. 1991a, Phys. Rev., D43, 3833
- Holman, R., Kolb, E.W., Vadas, S.L., & Wang, Y. 1991b, Phys. Lett., B269, 252
- Hu, W., Eisenstein, D.J., & Tegmark, M. 1997, preprint (astro-ph/9712057)
- Huey, G. & Dave, R. 1997, University of Pennsylvania preprint UPR-767T
- Jain, B., & Bertschinger, E. 1994, ApJ, 431, 495
- Jungman, G., Kamionkowski, M., Kosowsky, A., & Spergel, D.N. 1996, Phys. Rev., D54, 1332
- Kaiser, N. 1987, MNRAS, 227, 1
- Kofman, L., & Linde, A. 1987, Nucl. Phys. B282, 555
- Kamionkowski, M., Kosowsky, A., & Stebbins, A. 1997, Phys. Rev. Lett., 78, 2058
- Kauffman, G., Nusser, A., & Steinmetz, M. 1997, MNRAS, 286, 795
- Keating, B., Timbie, P., Polnarev, A. & Steinberger, J. 1998, ApJ, 495, 580
- Kendall, M.G. & Stuart, A. 1969, *The Advanced Theory of Statistics, Volume II*, Griffin, London
- Knox, L. 1995, Ph.D. Thesis, Univ. of Chicago

- Kolb, E.W. 1997, in *Current Topics in Astrofundamental Physics*, ed. N. Sanchez & Z. Zichichi (Singapore: World Scientific), 162
- Kolb, E.W., & Turner, M.S. 1990, *The Early Universe* (Addison-Wesley Publishing Company)
- La, D., & Steinhardt, P.J. 1991, *Phys. Rev. Lett.*, 62, 376
- Lesgourgues, J., Polarski, D., & Starobinsky, A.A. 1997, *Nuclear Physics B*, 497, 479
- Lidsey, J.E., Liddle, A.R., Kolb, E.W., Copeland, E.J., Barriero, T. & Abney, M. 1997, *Rev. Mod. Physics*, 69, 373
- Linde, A.D. 1983, *Phys. Lett.*, 129B, 177
- Lineweaver, C. & Barbosa, D. 1998, *A&A*, 329, 799
- Oh, S.P., Spergel, D.N. & Hinshaw, G. 1998, preprint (astro-ph/9805339)
- Peacock, J.A. 1997, *MNRAS*, 284, 885
- Peacock, J.A., & Dodds, S.J. 1996, *MNRAS*, 280, L19
- Peebles, P.J.E. 1993, *Principles of Physical Cosmology* (Princeton: Princeton University Press)
- Refregier, A. et al. 1998, preprint (astro-ph/9806349)
- Scherrer, R.J., & Weinberg, D.H. 1997, preprint (astro-ph/9712192)
- Seljak, U. 1996, *ApJ*, 482, 6
- Seljak, U., & Zaldarriaga, M. 1996, *ApJ*, 469, 437
- Spergel, D.N. 1994, *BAAS*, 26, 1427
- Strauss, M.A. 1997, in *Formation of Structure in the Universe*, edited by Avishai Dekel and Jeremiah P. Ostriker (Cambridge: Cambridge University Press), in press
- Tegmark, M. 1997, *Phys. Rev. Lett.*, 79, 3806
- Tegmark, M., Hamilton, A.J.S., Strauss, M.A., Vogeley, M.S., & Szalay, A.S. 1998, *ApJ*, 499, 555
- Tegmark, M., Taylor, A. & Heavens, A. F. 1997, *ApJ*, 480, 22
- Turner, M.S. 1997, in *Generation of Cosmological Large-Scale Structure*, ed. D.N. Schramm & P. Galeotti (Dordrecht: Kluwer), 153

- Turner, M.S., & Wang, Y. 1996, *Phys. Rev.*, D53, 5727
- Wang, Y. 1994, *Phys. Rev.*, D50, 6135
- Wang, Y. 1996, *Phys. Rev.*, D53, 639
- Webster, M., Hobson, M.P., Lasenby, A.N., Lahav, O., & Rocha, G. 1998, preprint (astro-ph/9802109)
- Weinberg, D. H. 1995, in *Wide-Field Spectroscopy and the Distant Universe*, eds. S. J. Maddox and A. Aragón-Salamanca (Singapore: World Scientific), 129
- Zaldarriaga, M., & Seljak, U. 1997, *Phys. Rev.*, D55, 1830
- Zaldarriaga, M., Spergel, D.N., & Seljak, U. 1997, *ApJ*, 488, 1

Fig. 1.— The confidence contours (68.3% and 95.4%) in the Ω_b - h (a) and Ω_m - h (b) planes assuming the SCDM model. The dotted lines are for MAP temperature data only, the dashed lines are for SDSS data to $k_{max} = 0.5 h\text{Mpc}^{-1}$ only, and the solid lines are for the combined MAP temperature and SDSS data.

Fig. 2.— The confidence contours (68.3% and 95.4%) in the Ω_Λ - Ω_m plane for the Λ CDM model. The line types are the same as in Figure 1.

Fig. 3.— The confidence contours (68.3% and 95.4%) in the τ_{ri} - C_2 plane for the SCDM model. The line types are the same as in Figure 1.

Fig. 4.— The primordial power spectrum with $1-\sigma$ error bars for MAP temperature data only (a), SDSS data only (b), and MAP temperature and SDSS data combined (c), assuming that the cosmological parameters are known to be that of the SCDM model (with $A_S^2(k) = 1$) listed in Table 1. The error bars in (b) which extend to the edges of the figure are infinite, as these refer to measurements of the power spectrum on scales larger than those which SDSS probes.

Fig. 5.— The primordial power spectrum with $1-\sigma$ error bars. (a) Combined MAP temperature and polarization data, with four cosmological parameters (h , Ω_Λ , Ω_b , τ_{ri}) included in the parameter estimation; (b) Combined MAP temperature and SDSS data, with five cosmological parameters (h , Ω_Λ , Ω_b , τ_{ri} , b) included in the parameter estimation.

Fig. 6.— The primordial power spectrum of Equation (23) with $1-\sigma$ error bars for the combined MAP temperature and SDSS data.

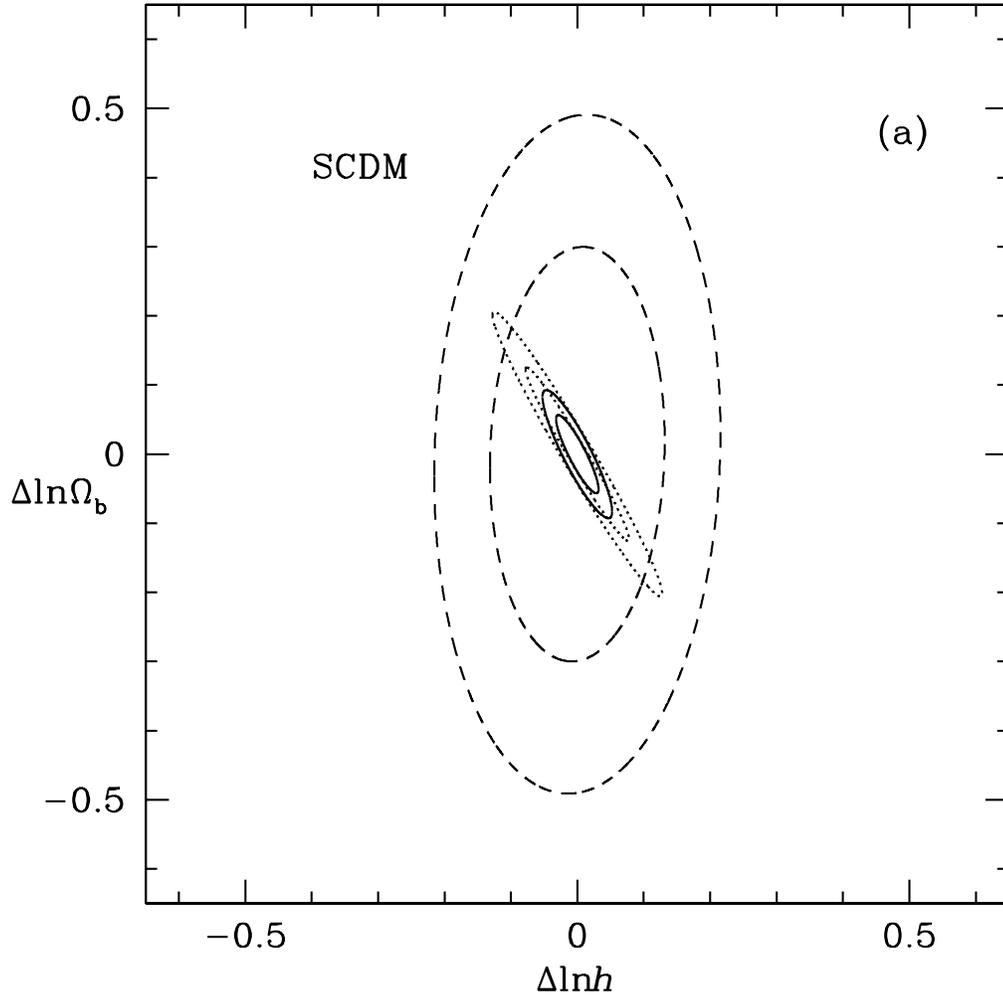


Fig. 1.— (a) The confidence contours (68.3% and 95.4%) in the Ω_b - h plane assuming the SCDM model. The dotted lines are for MAP temperature data only, the dashed lines are for SDSS data to $k_{max} = 0.5 h\text{Mpc}^{-1}$ only, and the solid lines are for the combined MAP temperature and SDSS data.

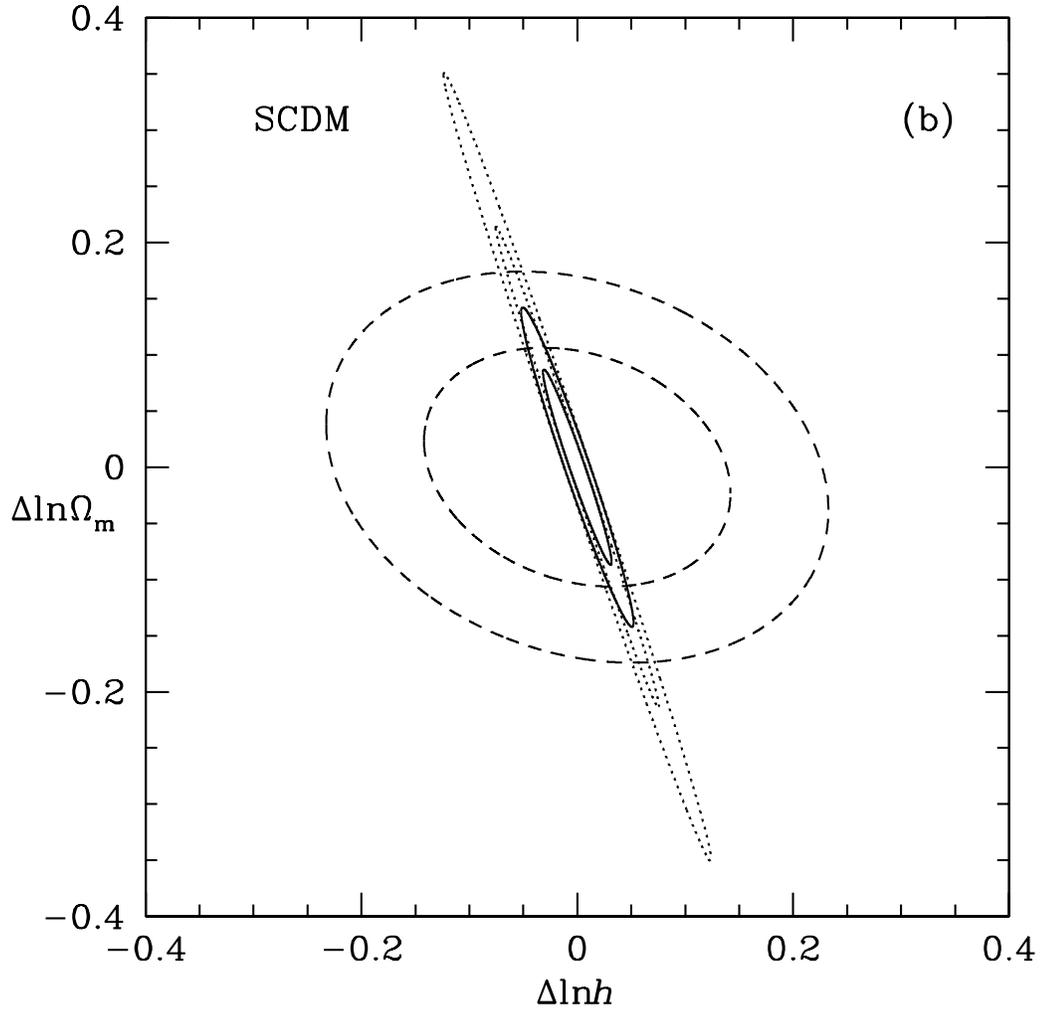


Fig. 1.— (b) The confidence contours (68.3% and 95.4%) in the Ω_m - h plane. The line types are the same as in (a).

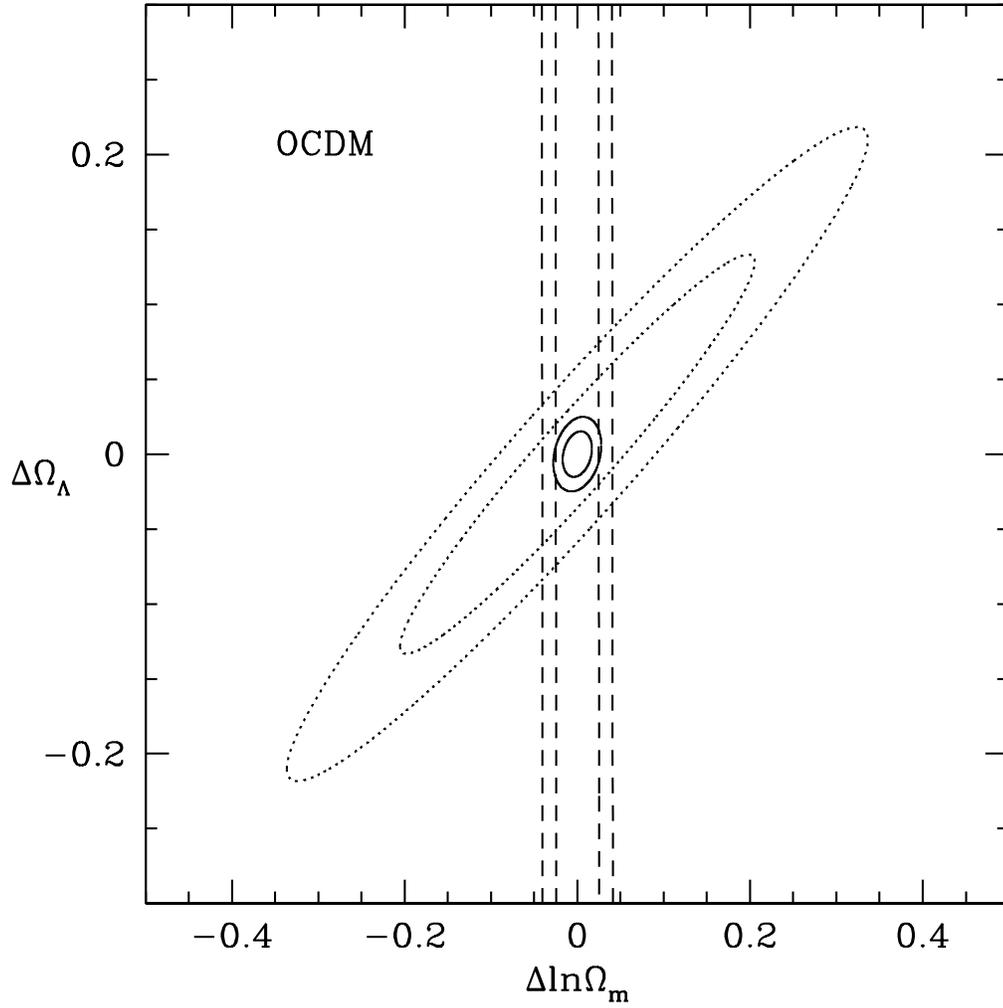


Fig. 2.— The confidence contours (68.3% and 95.4%) in the Ω_Λ - Ω_m plane for the OCDM model. The line types are the same as in Figure 1.

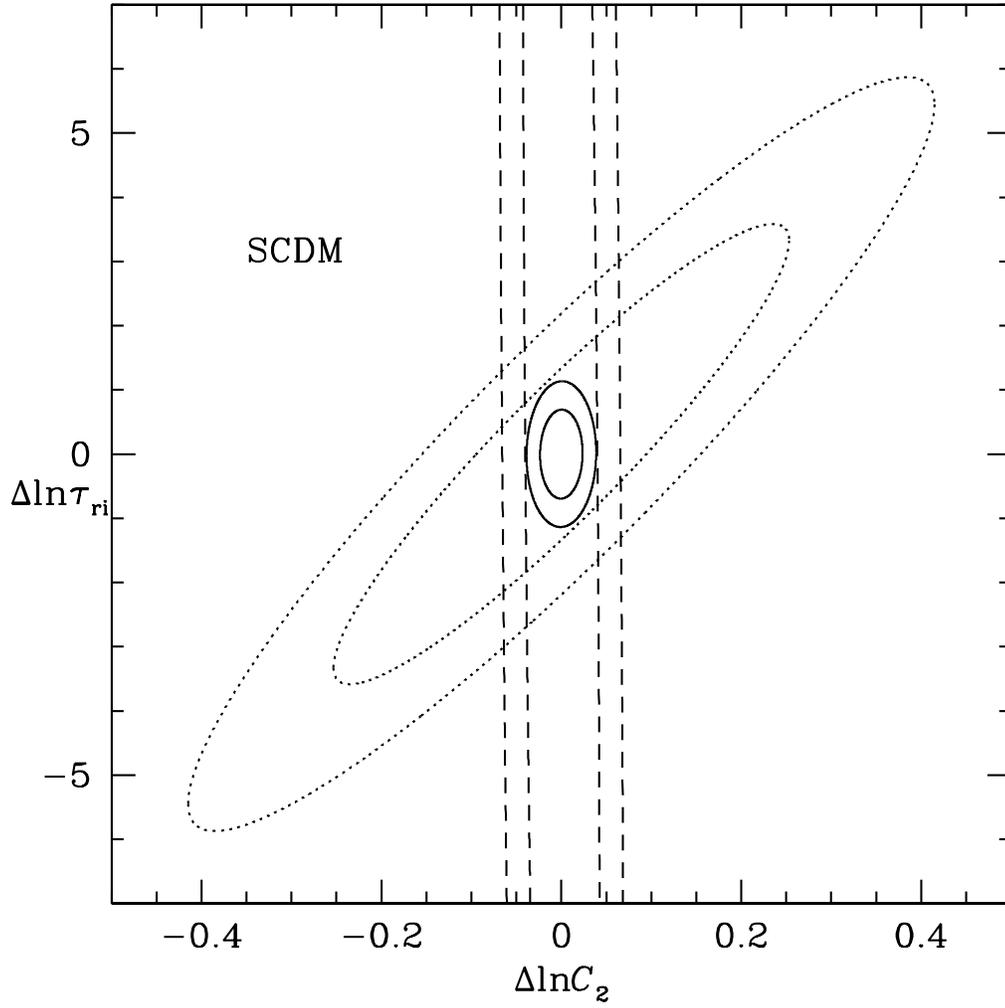


Fig. 3.— The confidence contours (68.3% and 95.4%) in the τ_{ri} - C_2 plane for the SCDM model. The line types are the same as in Figure 1.

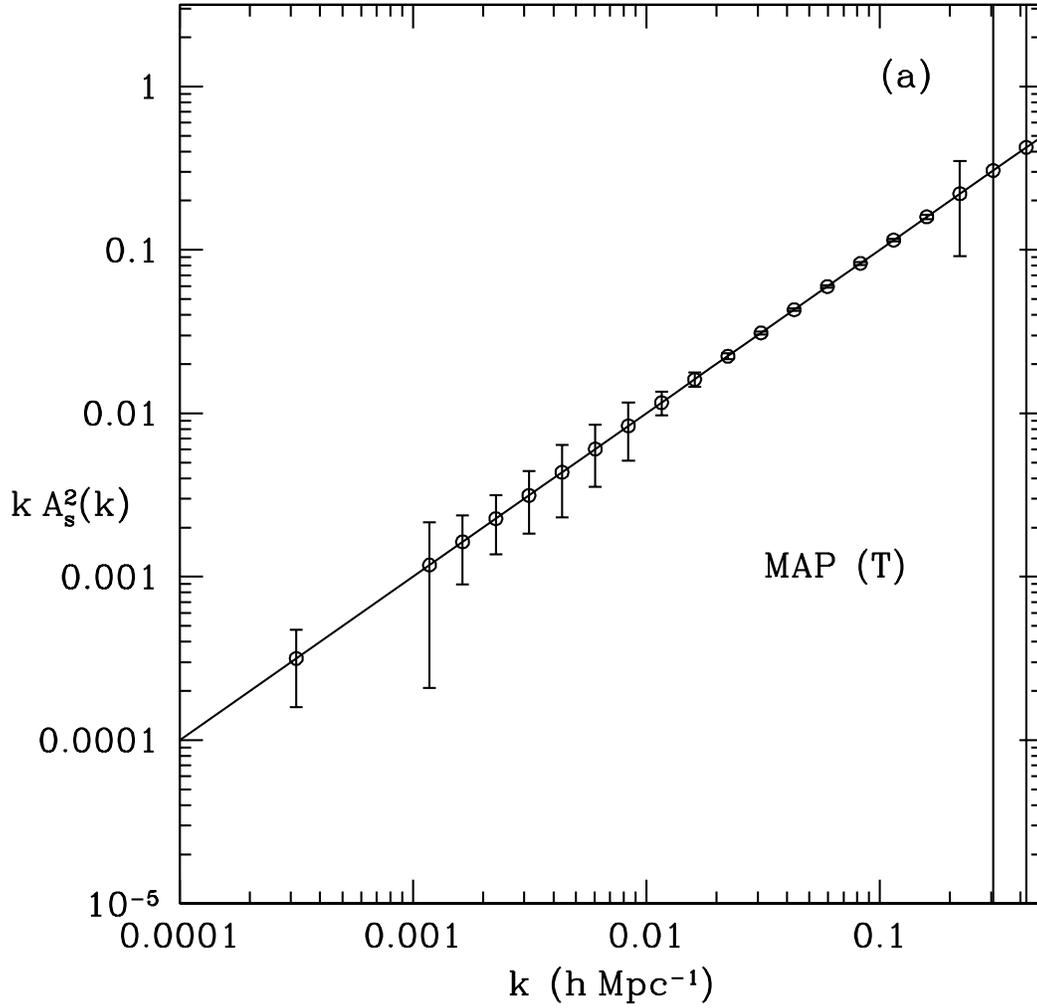


Fig. 4.— The primordial power spectrum with $1\text{-}\sigma$ error bars, assuming that the cosmological parameters are known to be that of the SCDM model (with $A_s^2(k) = 1$) listed in Table 1. (a) MAP temperature data only.

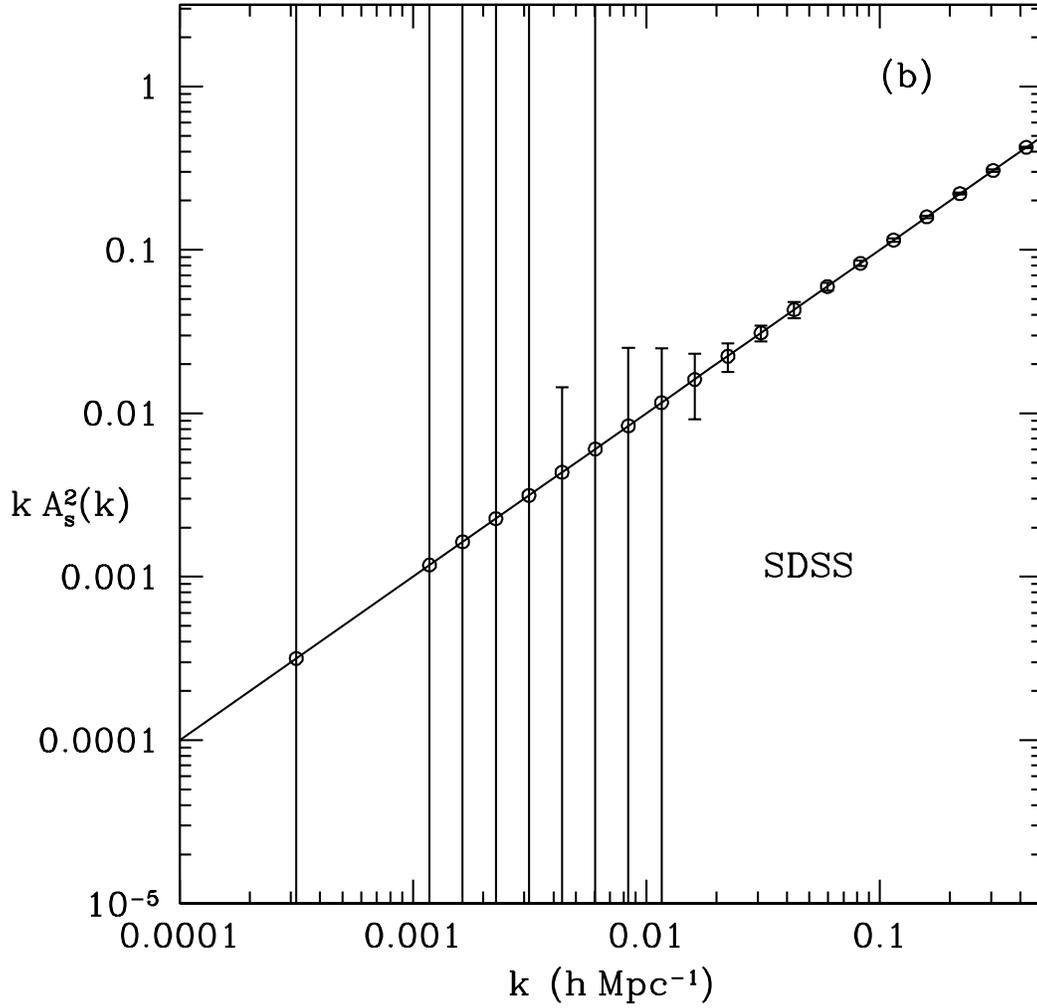


Fig. 4.— (b) SDSS data only. The error bars which extend to the edges of the figure are infinite, as these refer to measurements of the power spectrum on scales larger than those which SDSS probes.

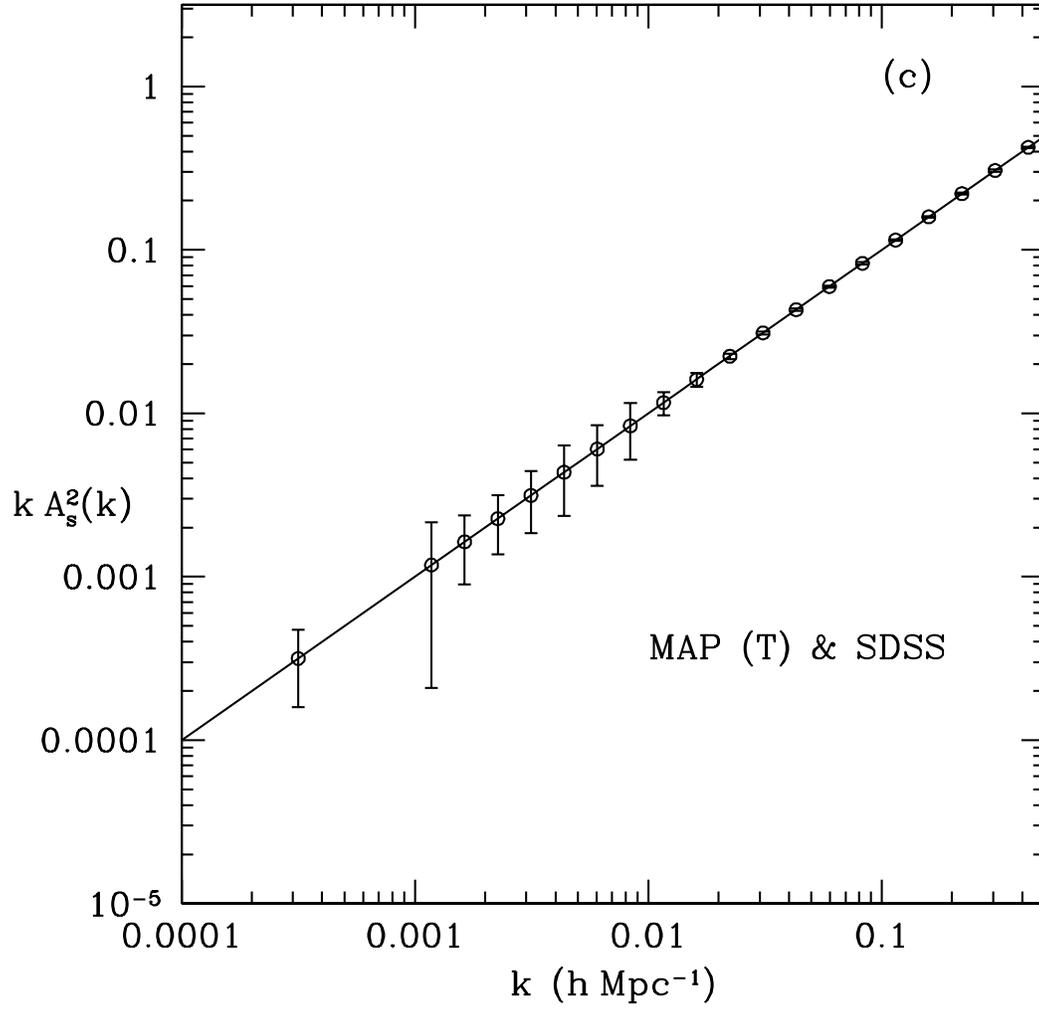


Fig. 4.— (c) MAP temperature and SDSS data combined.

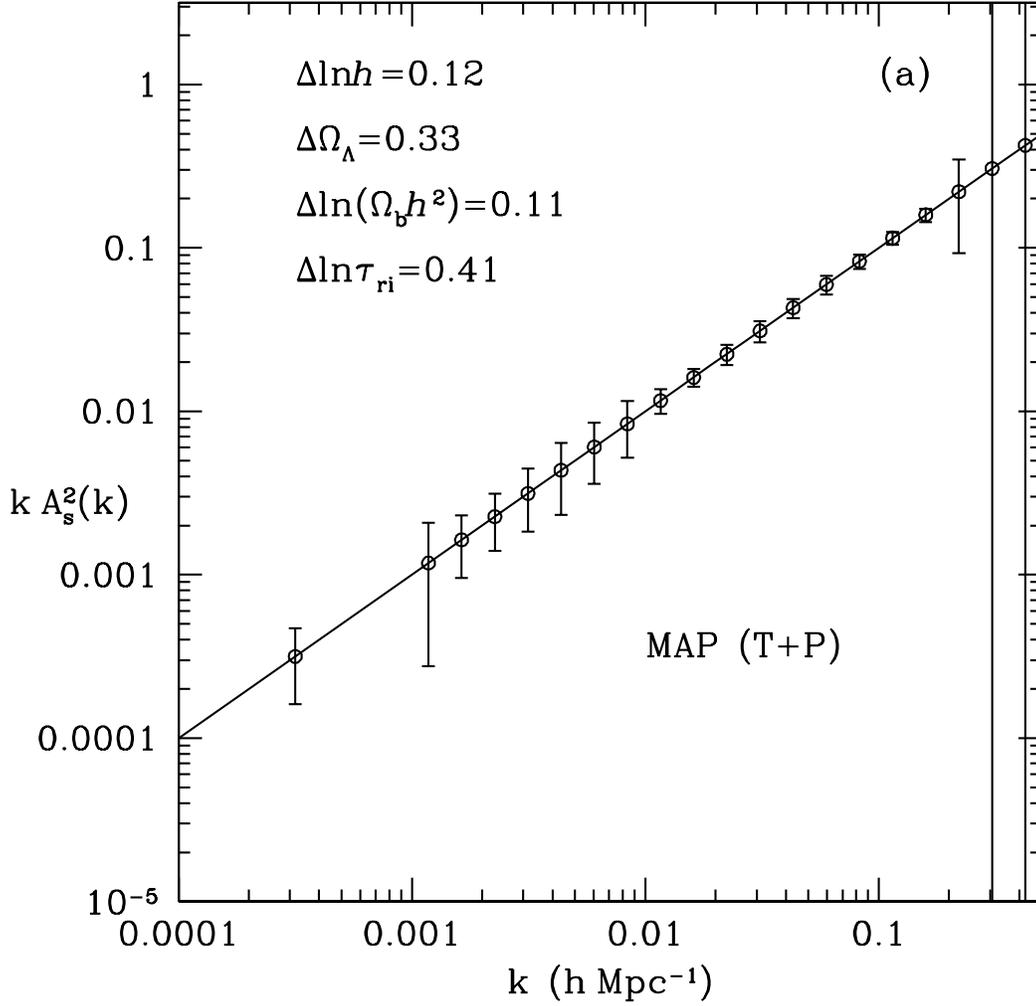


Fig. 5.— The primordial power spectrum with $1\text{-}\sigma$ error bars. (a) Combined MAP temperature and polarization data, with four cosmological parameters (h , Ω_Λ , Ω_b , τ_{ri}) included in the parameter estimation.

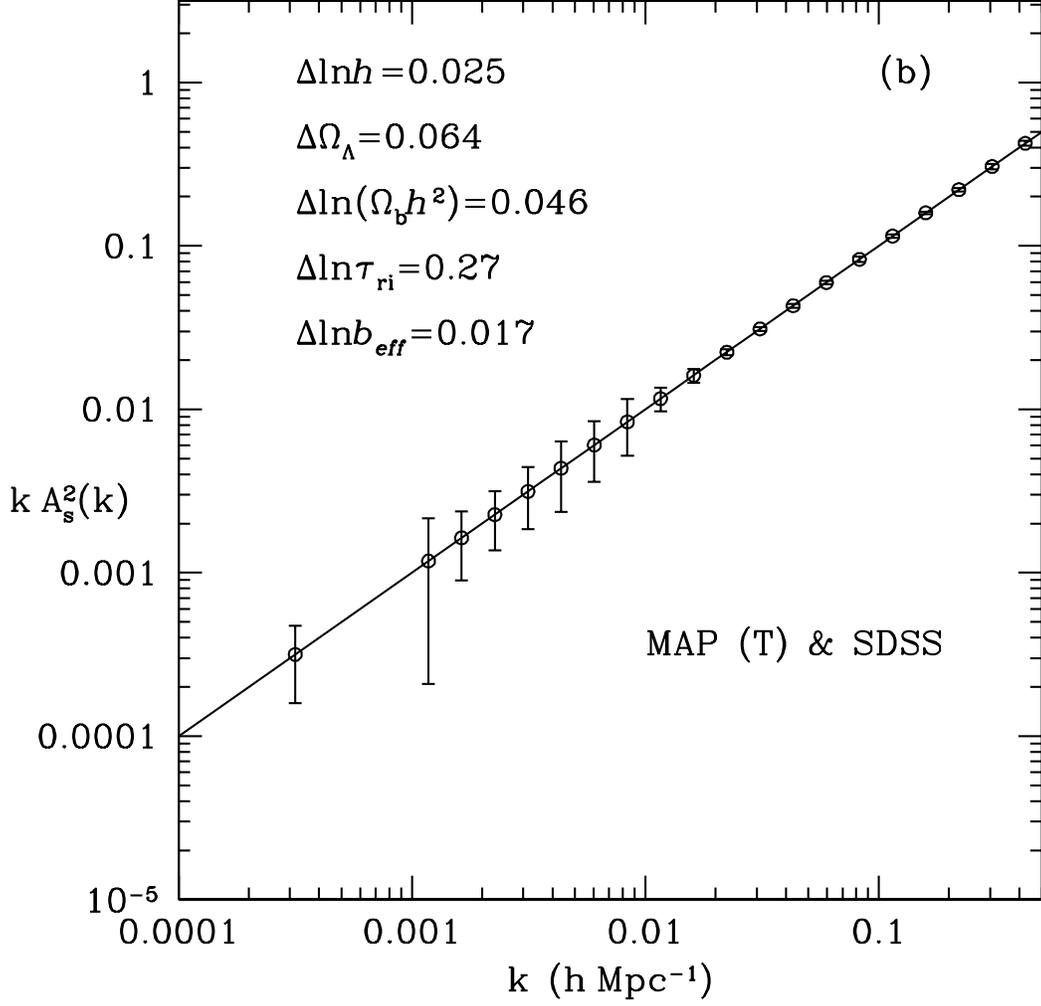


Fig. 5.— (b) Combined MAP temperature and SDSS data, with five cosmological parameters (h , Ω_Λ , Ω_b , τ_{ri} , b) included in the parameter estimation.

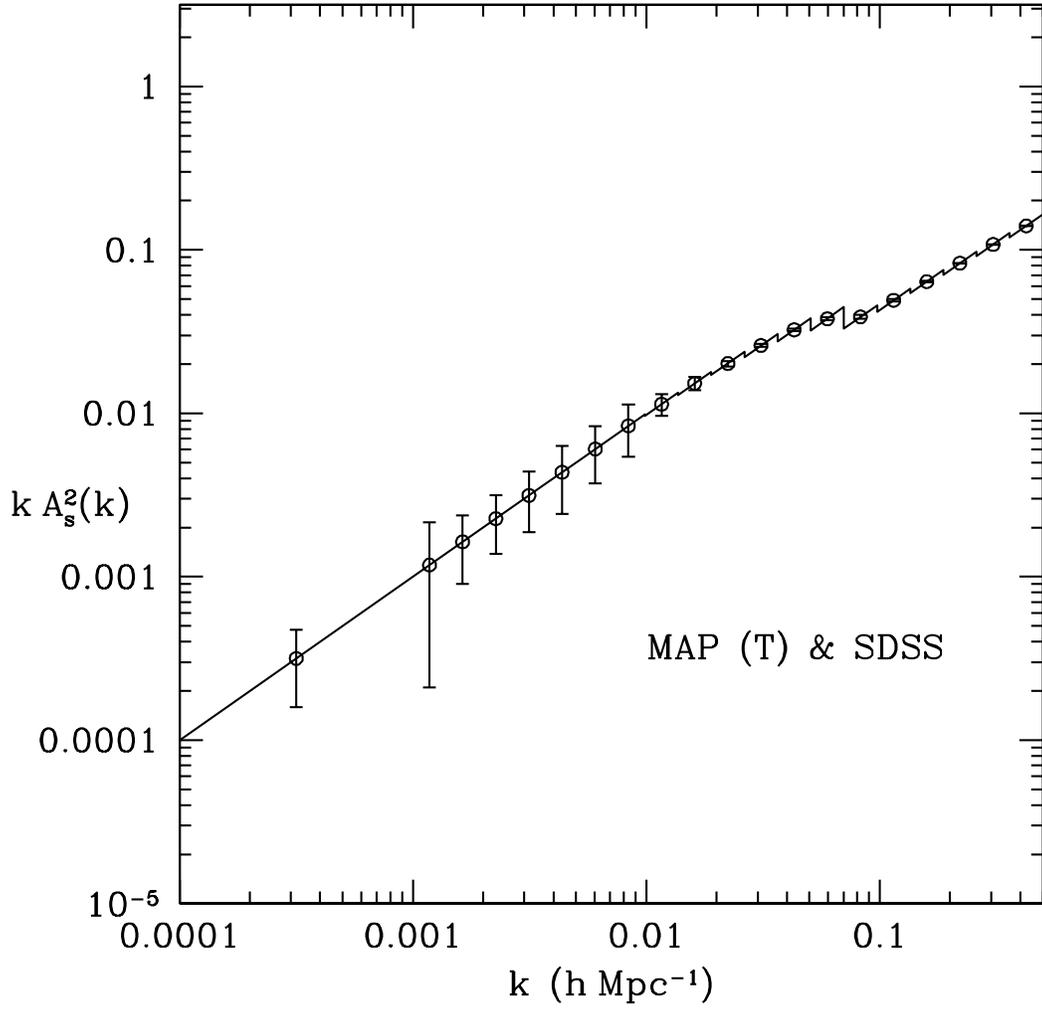


Fig. 6.— The primordial power spectrum of Equation (23) with $1\text{-}\sigma$ error bars for the combined MAP temperature and SDSS data.